ISSN 1674-1056
http://cpb.iphy.ac.cn
http://iopscience.iop.org/cpb
中国物理 B
Chinese Physics
中国物理
Chinese Physics B

rapid and convenient experimental method of absolutely calibrating transmission of x-ray flat-response filter

Jian Yu(余建), Li-Fei Hou(候立飞), Jing Wang(王静), Wen-Hai Zhang(张文海), Ming Chen(陈铭), Bao-Chong Zhou(周保充), Sha-Li Xiao(肖沙里), Shen-Ye Liu(刘慎业)
Citation: Chin. Phys. B . 2018, 27(10): 100702. **doi:** 10.1088/1674-1056/27/10/100702

Journal homepage: http://cpb.iphy.ac.cn; http://iopscience.iop.org/cpb

What follows is a list of articles you may be interested in

Nested grazing incidence optics for x ray detection

Lin-Sen Li(李林森), Peng-Fei Qiang(强鹏飞), Li-Zhi Sheng(盛立志), Yong-An Liu(刘永安), Zhe Liu(刘哲), Duo Liu(刘舵), Bao-Sheng Zhao(赵宝升), Chun-Min Zhang(张淳民)
Chin. Phys. B . 2017, 26(10): 100703. **doi:** 10.1088/1674-1056/26/10/100703

Property of slice square polycapillary x-ray optics

Shi-Qi Peng(彭诗棋), Zhi-Guo Liu(刘志国), Tian-Xi Sun(孙天希), Kai Wang(王锴), Long-Tao Yi(易龙涛), Kui Yang(杨魁), Man Chen(陈曼), Jin-Bang Wang(王金榜)
Chin. Phys. B . 2016, 25(2): 024102. **doi:** 10.1088/1674-1056/25/2/024102

Electrically tunable holographic polymer templated blue phase liquid crystal grating

He Zheng-Hong, Chen Chao-Ping, Zhu Ji-Liang, Yuan Ya-Chao, Li Yan, Hu Wei, Li Xiao, Li Hong-Jing, Lu Jian-Gang, Su Yi-Kai
Chin. Phys. B . 2015, 24(6): 064203. **doi:** 10.1088/1674-1056/24/6/064203

Polycapillary X-ray lens for secondary focusing Beijing synchrotron radiation source

Li Yu-De, Lin Xiao-Yan, Liu Shi-Gang, He Jin-Long, Guo Fei, Sun Tian-Xi, Liu Peng
Chin. Phys. B . 2013, 22(4): 044103. **doi:** 10.1088/1674-1056/22/4/044103

A rapid and convenient experimental method of absolutely calibrating transmission of x-ray flat-response filter*

Jian Yu(余建)[1], Li-Fei Hou(候立飞)[2], Jing Wang(王静)[2], Wen-Hai Zhang(张文海)[2,†], Ming Chen(陈铭)[2], Bao-Chong Zhou(周保充)[2], Sha-Li Xiao(肖沙里)[3], and Shen-Ye Liu(刘慎业)[2]

[1] *Key Laboratory of Optoelectronic Devices and Systems of Ministry of Education and Guangdong Province, College of Optoelectronic Engineering, Shenzhen University, Shenzhen* 518060, *China*

[2] *Research Center of Laser Fusion, China Academy of Engineering Physics, P.O. Box* 919-986, *Mianyang* 621900, *China*

[3] *College of Optoelectronic Engineering, Chongqing University, Chongqing* 400044, *China*

(Received 15 March 2018; revised manuscript received 6 June 2018; published online 10 September 2018)

We develop a rapid and convenient experimental method of absolutely calibrating the transmission of an x-ray flat-response filter. The calibration experiment is performed on a small laser-target facility, and a set of high resolution holographic flat-field grating spectrometers is used as a discrimination system of the laser-produced x-ray source. Given that the holographic flat-field grating has a relatively large width, the grating is divided into two regions for use in that direction, where one region has the filter added and the other region does not. The filter transmission is determined by dividing the x-ray signal counts detected when the filter is in the line of sight by those detected when the filter is out of the line of sight. We find that the calibration results of this experiment agree with the calibration results using a synchrotron radiation source, as well as simulation results. Our method is not only highly reliable but also rapid and convenient.

Keywords: flat-response filter, absolute transmission, flat-field grating spectrometer, x-ray CCD camera

PACS: 07.85.Fv, 41.50.+h, 42.40.Eq, 42.62.Fi **DOI:** 10.1088/1674-1056/27/10/100702

1. Introduction

Indirect drive inertial confined fusion (ID ICF) is one of the main fusion ICF schemes.[1–4] The x-ray filters have been extensively used in the research field of ID ICF for blocking target debris, eliminating stray light, or attenuating the x-ray signal intensity.[5–7] However, due to their positions that just face to the chamber center, x-ray filters are often destroyed by target debris or contaminated by oil molecules. Thus, x-ray filters need to be calibrated regularly to obtain a real transmission value. The synchrotron radiation source is very suitable for calibrating filter transmission because of its characteristic wide spectral range, good brightness, and monochromaticity, and the corresponding calibration accuracy is quite high.[5,8] However, there are also many disadvantages: the beam line availability and the logistics of setting up the experiment usually take several weeks to months,[8,9] and the fixed location and fixed size of different devices of the synchrotron radiation facility and the beam uniformity severely constrain the size and location of the x-ray filter, which can be calibrated.[10,11] In addition, a Henke source can also be considered as a source for calibrating filter transmission.[7,12,13] Unfortunately, the anode material, electrical system limitations, and secondary fluorescent materials limit the intensity of the source, which leads to a low calibration accuracy.[5,9] An electron beam ion trap facility can also be used as an excellent x-ray source for calibrating x-ray filters. Brown *et al.* performed an x-ray blocking filter calibration experiment on the electron beam ion trap facility at the Lawrence Livermore National Laboratory.[9] The calibration accuracy of the experiments is good, however, there are relatively few electron beam ion trap facilities in some countries.

In recent years, many researchers have been attracted by laser-produced x-ray sources due to their high intensity and easy availability.[11,14] Using a laser-produced x-ray source coupled with various types of dispersion systems, many devices such as streak cameras,[15] x-ray CCD cameras,[16] and grating spectrometers[17] have been absolutely calibrated. Mirror-filters[18] and transmission grating spectrometers[19] are the two most commonly selected dispersion systems for these calibration experiments. To the best of our knowledge, no results have yet been reported on the calibration of a filter's transmission based on a laser-produced x-ray source. In this paper, we introduce in detail a filter transmission calibration experiment on a small laser-target facility. We choose the novel compound filter developed by our research team as the calibration object of this experiment.[10] Here, the novel compound filter consists of two Au foils, with thickness values of 0.05 μm and 0.4 μm, respectively. The 0.4-μm foil consists of an array of pinholes each with a diameter of 5 μm and a distance of 11 μm between the pinholes. In this paper, we refer to the novel compound filter as a flat-response filter. Given

*Project supported by the National Natural Science Foundation of China (Grant Nos. 11405158 and 11775203) and the Presidential Foundation of China Academy of Engineering Physics (Grant No. YZJJLX 2016007).

†Corresponding author. E-mail: xiaoyuercqu@sina.cn

© 2018 Chinese Physical Society and IOP Publishing Ltd

that traditional dispersion systems (mirror-filters and transmission grating spectrometers) have a low spectral resolution and cumbersome spectra unfolding process, we choose a set of high resolution holographic flat-field grating spectrometers as the discrimination system of the laser-produced x-ray source. The holographic flat-field grating can suppress higher order diffraction effectively so that the detected signal in our calibration experiment does not need a cumbersome spectra unfolding process. In view of the fact that the holographic flat-field grating has a large width, the grating is divided into two regions. In one region we add the flat-response filter, and in the other region nothing is added. The filter transmission can be determined by dividing the x-ray signal counts detected in the region where the filter is in the line of sight by those detected in the region where the filter is out of the line of sight. The rest of this article is organized as follows. We first introduce in detail the experimental setup in Section 2. Then, we present the calibration results of this experiment and the data analysis in Section 3. Finally, we briefly summarize the advantages of the proposed method in Section 4.

2. Experimental setup

The calibration experiments were performed on a 100-J laser facility at the Research Center of Laser Fusion of the Chinese Academy of Engineering Physics, and the schematic diagram of the experiment setup is shown in Fig. 1. A laser pulse of 1053-nm light which had a full-width at half-maximum of 4 ns was focused into a 250-μm-diameter spot and irradiates a planar polyimide ($C_{16}H_6O_4N_2$) membrane target at normal incidence. In this experiment, the laser energy was set to be 63 J. The holographic flat-field grating spectrometer consisted of an incident slit with 62 μm in width and 2.5 cm in length, a holographic flat-field grating with a line density of 2400 l/mm at the grating center, and an Andor x-ray CCD camera with a pixel size of 13.5 μm. The spectrometer detected a signal from various wavelength x-ray photons at 45 °C with respect to the incident laser direction. Figure 2 gives the details of the setup of the holographic flat-field grating spectrometer and the location of the flat-response filter. The gratings were gold-coated and designed to be used at a grazing incidence angle of 88.6 °C. The effective length of the flat focal plane was 26.8 mm and the corresponding wavelength range was from 10 Å to 70 Å (the corresponding energy ranges from 177 eV to 1.24 keV). The holographic flat-field grating was commercially available from Shimadzu Corporation, and its length, width and height were 50, 30, and 10 mm, respectively. Due to the relatively large width, the grating was divided into two regions. We note that this calibration method did not depend on the knowledge of the holographic flat-field grating efficiency because the diffraction efficiencies of the divided two regions on the surface of the grating could be considered to be equal. In the first region, the filter tightly adhered to the front end of the grating, and in the second region nothing was added. The specific location of the filter can be seen clearly in Fig. 2. On the flat focal plane, region I corresponds to the spectrum signal with the filter, and region II corresponds to the signal without the filter. The x-ray CCD camera was of a 2048 × 2048 array, with an image area of 27.6 mm×27.6 mm, which was large enough to receive the signals of the two regions simultaneously. The signal acquisition time of the x-ray CCD was 10 ns. The distance from the entrance slit to the grating center was 236.7 mm and the distance from the grating center to the flat field plane was 235 mm. The angle between the grating normal and the horizontal plane was 90.5 °C, and the x-ray CCD was placed at the flat focal plane.

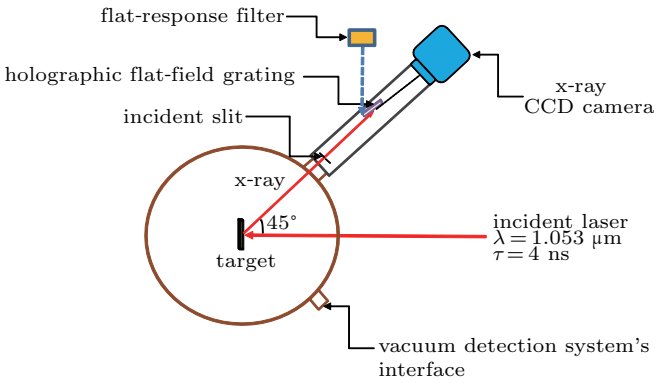


Fig. 1. (color online) Schematic diagram of calibration experiment.

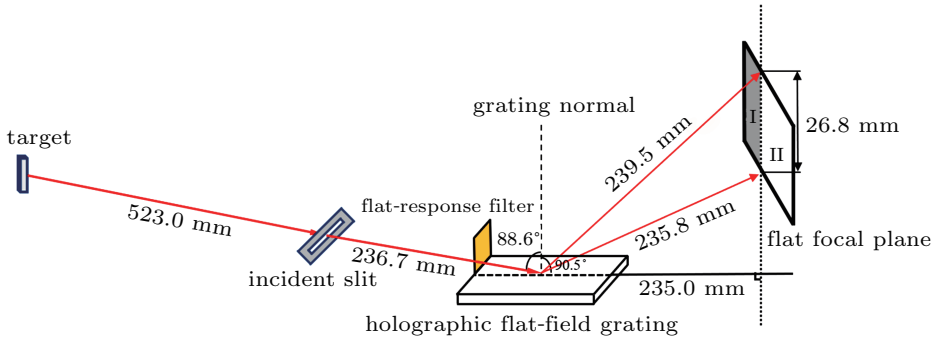


Fig. 2. (color online) Detailed setup of holographic flat-field grating spectrometer and location of the flat-response filter.

3. Results and data analysis

Figure 3 shows the two local images obtained by the CCD camera in region I and region II, where the red arrow indicates the direction of spectral dispersion. Figure 3(a) corresponds to region I where the spectrum signal is filtered by the flat-response filter, and figure 3(b) corresponds to region II where the spectrum signal is not filtered by the filter. After the attenuation of the filter, the intensity of spectrum signal is noticeably weakened. The spectrum profile contains much characteristic radiation and a small amount of bremsstrahlung radiation in the spectral region of our concern. In fact, these characteristic spectral lines are mainly the H-like and He-like resonance lines of the C, N, and O elements according to Ref. [20]. In this paper, we only take the line spectral composition as a research objective because the bremsstrahlung radiation is very weak in the spectral region of our concern.

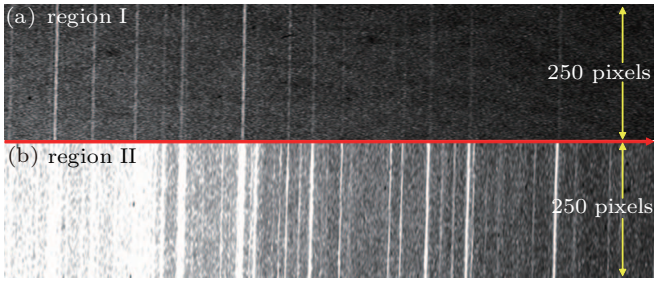


Fig. 3. (color online) Images obtained from two different regions on the flat focal plane: (a) region I and (b) region II.

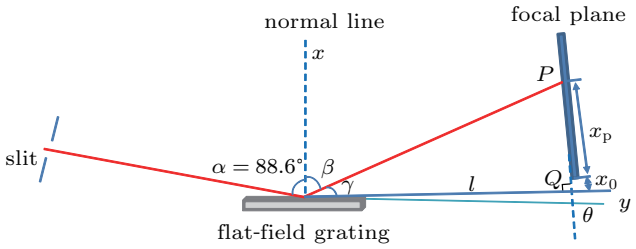


Fig. 4. (color online) Layout diagram of holographic flat-field grating under real experimental conditions.

Given that the x-ray transmission of the flat-response filter is wavelength dependent, we first need to identify the wavelengths of these spectral lines. Here, the wavelengths of several strong lines can be identified by using the National Institute of Standards and Technology's (NIST) Atomic Spectra Database[20] or the results of the part identified in Ref. [20]. According to the above two methods, however, it is difficult to identify the wavelengths of all spectral lines. According to several spectral lines, we precisely calibrate the relationship between the x-ray wavelength and the pixel position on the x-ray CCD by using the proposed parameter fitting method in Ref. [20]. In Fig. 2, the experimental parameter configuration is an ideal case. However, the actual parameters may deviate from the nominal value due to some complex influencing factors. Figure 4 shows a more universal configuration where θ is not restricted to 90 °C.

According to the geometry relationship in Fig. 3, it is not difficult to deduce the relationship between the wavelength and the pixel position as follows:

$$\lambda = d_0\Bigg(\sin\alpha - \sin\Bigg(0.5^\circ + \theta - \arctan\Bigg(\tan\Bigg(0.5^\circ + \theta - \arcsin\Bigg(\sin\alpha - \frac{\lambda_C}{d_0}\Bigg)\Bigg) + \frac{(p - p_C)\,s}{l}\Bigg)\Bigg)\Bigg), \tag{1}$$

where λ is the wavelength, p is the pixel position corresponding to wavelength λ, d_0 is the nominal spacing at the grating center, α is the incident angle, l is the distance between the grating center and the focal plane, and λ_C and p_C are the wavelength and position of any identified line, respectively. With multiple identified wavelengths and pixel values, we can obtain all spectral line wavelengths at different pixel positions by fitting with the above equation.

As shown in Fig. 3, the length of 250 pixels near the center area is chosen as the signal count range in the two different regions, separately. Meanwhile, using the relationship between the wavelength and the pixel position, the signal counts at different wavelengths can be obtained. Figures 5(a) and 5(b) show the signal counts at different wavelengths in the different regions, where the bremsstrahlung radiation and background noise have been subtracted. As shown in Fig. 5, the intensity counts of the spectrum signal are noticeably weakened after the attenuation of the flat-response filter. By measuring the full widths at half maximum (FWHMs) of all spectral lines in Figs. 5(a) and 5(b), we can see that the spectral resolution in each of region I and region II maintains consistence to a high degree. In the whole measured spectral range, the spectral resolution of the holographic flat-field grating spectrometer is better than 0.24 Å. Generally, the high spectral resolution is sufficient to distinguish the line spectrum structure of common target material. Through these data in Fig. 5, the x-ray transmissions for different wavelengths each can be determined by dividing the x-ray signal counts detected within the 250 pixels in region I by those detected in region II. The transmission of the flat-response filter can be expressed as follows:

$$T(\lambda) = \frac{C_{\mathrm{I}}(\lambda)}{C_{\mathrm{II}}(\lambda)}, \tag{2}$$

where $T(\lambda)$ represents the x-ray transmission value at a given wavelength λ, $C_{\mathrm{I}}(\lambda)$ denotes the total response counts corresponding to region I, and $C_{\mathrm{II}}(\lambda)$ refers to the total response counts corresponding to region II.

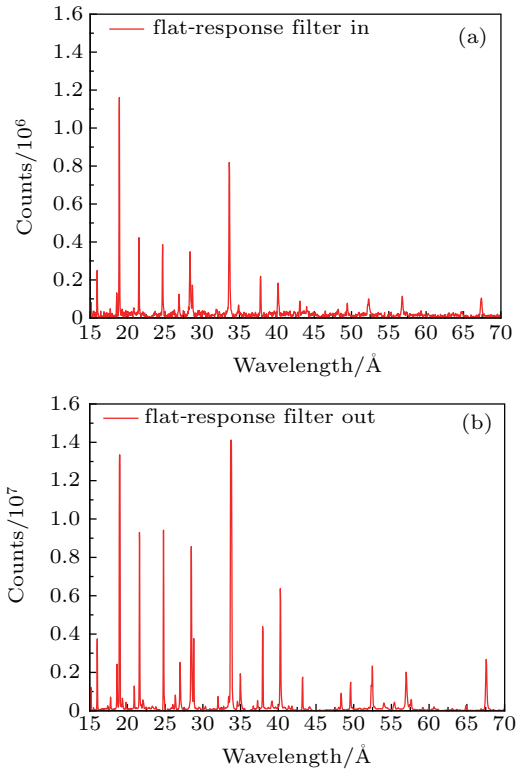


Fig. 5. (color online) Signal counts at different wavelengths for (a) region I and (b) region II.

Figure 6 shows the calibrated results of this experiment. The calibrated results are obtained by using the Beijing synchrotron radiation source, as well as the simulation results. The red square data points represent the absolute transmission of the flat-response filter obtained from this experiment, while the vertical bars show the measurement uncertainty due to statistical error and an estimate of the systematic error. The green circle data points represent the calibration results obtained by using the synchrotron source, and the blue triangle data points show the simulation results for the designed thickness and duty ratio of Au by using a MATLAB code written by our team.

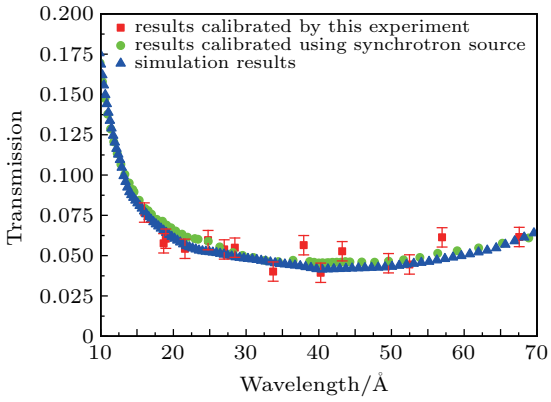


Fig. 6. (color online) Several results from different approaches. Red squares: calibration results in this experiment (vertical bars show measurement uncertainty). Green circles: results obtained using Beijing synchrotron radiation source. Black triangles: simulation results.

Comparing these three results, we find that the calibration results of this experiment are in good agreement with the results obtained using the Beijing synchrotron radiation source and with the simulation results in the whole spectral region. Some data points in the results of this experiment deviate slightly from the results obtained using the synchrotron radiation source and also from the simulation results. It is not clear yet what causes this deviation. It may be attributed to the consistency of the width at different locations on the entrance slit. In addition, the selection of the subtracted background noise and bremsstrahlung radiation counts in data processing might be the reason. However, the deviation is small with respect to the experimental results obtained using the synchrotron source and the simulation results. Hence, our calibration method can also achieve high accuracy.

4. Conclusions

We have performed a transmission calibration experiment for a flat-response filter on a small laser-target facility. A set of holographic flat-field grating spectrometers is used as a dispersion system for the laser-produced x-ray source. Taking advantage of the width, the flat-field grating is divided into two regions. The calibration experiment uses only one laser-target test, so the calibration efficiency is very high. The whole process of the experiment may only take an hour or less. Of course, the selection of the target is very important because the calibration experiment requires multiple line spectra to calibrate the transmission of multiple energy points. In addition, our experiment only needs one set of holographic flat-field grating spectrometers as the measurement system, so the experimental processing is also very convenient. Moreover, our measurement method can be generalized to other energy regions by using different holographic flat-field gratings. By comparing the corresponding results, we see that the calibration results of this experiment are in good agreement with the calibration results obtained using the synchrotron radiation source, as well as with the simulation results. Hence, this method can be considered as an alternative for high accuracy transmission calibration of flat-response filters. Unlike calibration experiments using a synchrotron source facility or an electron beam ion trap facility, our method removes experimental facility restrictions on the time and place of calibration because small laser facilities are more common.

Acknowledgment

All authors are very grateful to Xingsen Che for the x-ray flat-response filter preparation and Tuo Zhu for the useful discussion and advice on the experimental design. We also thank Professors Jiang Saoen and Yang Jiamin from the Laser Fusion Research Center and Prof. Wang Yiping from Shenzhen University for their support with experimental equipment and funding.

References

[1] Lindl J, Amendt P, Berger R, Glendinning S, Glenzer S, Haan S, Kauffman R, Landen O and Amendt P 2004 *Phys. Plasmas* **11** 339

[2] Shang W L, Betti R, Hu S X, Woo K, Hao L, Ren C, Christopherson A R, Bose A and Theobald W 2017 *Phys. Rev. Lett.* **119** 195001

[3] Shang W L, Yang J M and Dong Y S 2013 *Appl. Phys. Lett.* **102** 094105

[4] Theobald W, Bose A, Yan R, Betti R, Lafon M, Mangino D, Christopherson A R, Stoeckl C, Seka W, Shang W, Michel D T, Ren C, Nora R C, Casner A, Peebles J, Beg F N, Ribeyre X, Llor A E, Colaïtis A, Tikhonchuk V and Wei M S 2017 *Phys. Plasmas* **24** 120702

[5] Campbell K M, Weber F A, Dewald E L, Glenzer S H, Landen O L, Turner R E and Waide P A 2004 *Rev. Sci. Instrum.* **75** 3768

[6] Saemann A and Eidmann K 1998 *Rev. Sci. Instrum.* **69** 1949

[7] Hubert S, Dubois J L, Gontier D, Lidove G, Reverdin C, Soullie G, Stemmler P and Villette B 2010 *Rev. Sci. Instrum.* **81** 053501

[8] Bourgade J L, Villette B, Bocher J L, Boutin J Y, Chiche S, Dague N, Gontier D, Jadaud J P, Savale B and Worbel R 2001 *Rev. Sci. Instrum.* **72** 1173

[9] Brown G V, Beiersdorfer P, Emig J, Frankel M, Gu M F, Heeter R F, Magee E, Thorn D B, Widmann K, Kelley R L, Kilbourne C A and Porter F S 2008 *Rev. Sci. Instrum.* **79** 10E309

[10] Li Z, Jiang X, Liu S, Huang T, Zheng J, Yang J, Li S, Guo L, Zhao X, Du H, Song T, Yi R, Liu Y, Jiang S and Ding Y 2010 *Rev. Sci. Instrum.* **81** 073504

[11] Reverdin C, Paurisse M, Caillaud T, Combis P, Duval A, Gontier D, Husson D, Rubbelynck C and Zuber C 2008 *Rev. Sci. Instrum.* **79** 10E932

[12] Lazarchuk V P, Muntyan A N, Murugov V M, Petrov S I and Senik A V 1976 *Rev. Sci. Instrum.* **47** 255

[13] Audley M D, Arnaud K A, Gendreau K C, Boyce K R, Fleetwood C M, Kelley R L, Keski-kuha R A, Scott F, Stahle C K, Szymkowiak A E, Tveekrem J L, Fujimoto R, Mitsuda K, Ishisaki Y and Mihara T 1999 *Proc. SPIE* **3765** 751

[14] Perez F, Kemp G E, Regan S P, Barrios M A, Pino J, Scott H, Ayers S, Chen H, Emig J, Colvin J D, Bedzyk M, Shoup M J, Agliata A, Yaakobi B, Marshall F J, Hamilton R A, Jaquez J, Farrell M, Nikroo A and Fournier K B 2014 *Rev. Sci. Instrum.* **85** 11D613

[15] Kauffman R L, Stradling G, Attwood D T and Medecki H 1983 *IEEE J. Quantum Electron.* **19** 616

[16] Labate L, Galimberti M, Giulietti A, Giulietti D, Gizzi L A, Tomassini P and Cocco G D 2002 *Nucl. Instrum. Method A* **495** 148

[17] Saemann A and Eidmann K 1998 *Rev. Sci. Instrum.* **69** 1949

[18] Stradling G L, Attwood D T and Kauffman R L 1983 *IEEE J. Quantum Electron.* **19** 604

[19] Nakai M, Kondou K, Urasaki T, Sakurai K, Nishimura H, Izawa Y and Yamanaka C 1986 30*th Annual Technical Symposium. International Society for Optics and Photonics*, August 12, 1986, San Diego, USA, p. 144

[20] Xiong G, Zhang J, Yang G, Yang J, Li H, Hu Z, Zhao Y, Wei M and Yi T 2014 *Phys. Scr.* **89** 065005

[21] Kramida A, Ralchenko Y, Reader J and Team D 2013 NIST At. Spectra Database Version 5.1 (Gaithersburg, MD: National Institute of Standards and Technology) http://physics.nist.gov/asd